



LAWRENCE  
LIVERMORE  
NATIONAL  
LABORATORY

# Wavelength measurement of $n = 3 - n' = 3$ transitions in highly charged tungsten ions

J. Clementson, P. Beiersdorfer

March 16, 2010

Physical Review A

## **Disclaimer**

---

This document was prepared as an account of work sponsored by an agency of the United States government. Neither the United States government nor Lawrence Livermore National Security, LLC, nor any of their employees makes any warranty, expressed or implied, or assumes any legal liability or responsibility for the accuracy, completeness, or usefulness of any information, apparatus, product, or process disclosed, or represents that its use would not infringe privately owned rights. Reference herein to any specific commercial product, process, or service by trade name, trademark, manufacturer, or otherwise does not necessarily constitute or imply its endorsement, recommendation, or favoring by the United States government or Lawrence Livermore National Security, LLC. The views and opinions of authors expressed herein do not necessarily state or reflect those of the United States government or Lawrence Livermore National Security, LLC, and shall not be used for advertising or product endorsement purposes.

# Wavelength measurement of $n = 3 - n' = 3$ transitions in highly charged tungsten ions

J. Clementson\* and P. Beiersdorfer

*Lawrence Livermore National Laboratory, Livermore, California 94550, USA*

(Dated: March 10, 2010)

## Abstract

$3s_{1/2} - 3p_{3/2}$  and  $3p_{1/2} - 3d_{3/2}$  transitions have been studied in potassiumlike  $W^{55+}$  through neonlike  $W^{64+}$  ions at the electron-beam ion trap facility in Livermore. The wavelengths of the lines have been measured in high resolution relative to well known reference lines from oxygen and nitrogen ions. Using the high-energy SuperEBIT electron-beam ion trap and an  $R = 44.3$  m grazing-incidence soft x-ray spectrometer, the lines were observed with a cryogenic charge-coupled device camera. The wavelength data for the sodiumlike and magnesiumlike tungsten lines are compared with theoretical predictions for ions along the isoelectronic sequences.

---

\* Also at Atomic Physics Division, Lund University, SE-221 00 Lund, Sweden; electronic address [clementson@llnl.gov](mailto:clementson@llnl.gov)

## I. INTRODUCTION

Multi-electron ions of high- $Z$  elements are of interest in atomic structure theory [1]. Accurate modeling of these systems needs to include electron correlation and relativistic effects in addition to quantum electrodynamic (QED) corrections [2, 3]. Relativistic and QED effects are strongly dependent on the nuclear charge  $Z$ , which makes highly charged heavy ions suitable for investigations of high-order QED effects [4]. However, the problem of accurately calculating the structure of highly charged ions becomes challenging as the number of electrons increases. Among many-electron systems, ions with only a few valence electrons outside the last closed shell are the simplest, and those high- $Z$  ions isoelectronic to sodium and magnesium thus represent useful stepping stones for testing QED calculations in multi-electron systems.

The  $3s_{1/2} - 3p_{3/2}$  resonance transition along the sodium isoelectronic sequence has been calculated by several authors. For instance, Ivanov and Ivanova used a model potential method and extrapolated experimental data to high- $Z$  ions [5]. Kim and Cheng calculated the wavelengths for a few high- $Z$  ions using Dirac-Fock wave functions [6]. Johnson *et al.* performed relativistic many-body perturbation theory (RMBPT) calculations [7] from which Seely and Wagner calculated semi-empirical wavelengths [8]. Predictions were also given by Kim *et al.* after investigating relativistic electron-correlation energies [2]. Baik *et al.* performed single-configuration Dirac-Fock calculations [9], whereas Seely *et al.* calculated multi-configuration Dirac-Fock (MCDF) wavelengths [10]. Blundell added QED corrections to RMBPT calculations and studied the resonance transition for a few selected high- $Z$  ions [11]. Theoretical wavelengths for the resonance line of magnesiumlike spectra include MCDF calculations by Cheng and Johnson [12], relativistic random-phase approximation (RRPA) calculations by Shorer *et al.* [13], relativistic perturbation theory using a model-potential by Ivanova *et al.* [14], MCDF calculations of Marques *et al.* [15], relativistic configuration-interaction (RCI) calculations by Chen and Cheng [16], and multi-configuration Dirac-Hartree-Fock (MCDHF) of Zou and Froese Fischer [17].

Up to xenon ( $Z = 54$ ) the  $3s_{1/2} - 3p_{3/2}$  line has been measured for most ions isoelectronic to sodium, but for higher  $Z$  rather few measurements are reported [10, 18–23]. Experimental high-precision wavelengths for the corresponding transition in magnesiumlike high- $Z$  ions are even less common [18, 19, 22]. Chen *et al.* measured the  $3s_{1/2} - 3p_{3/2}$  transition in P-

like through Na-like U at the Livermore EBIT-I electron-beam ion trap and found excellent agreement with RCI calculations [24]. Recently, Gillaspy *et al.* measured the  $3s_{1/2} - 3p_{3/2}$  and the  $3s_{1/2} - 3p_{1/2}$  transitions in Na-like high- $Z$  ions, including tungsten, together with the  $3s_{1/2} - 3p_{3/2}$  transition in Mg-like and the  $3p_{1/2} - 3d_{3/2}$  transition in Al- and Si-like ions, at the electron-beam ion trap facility at the National Institute of Standards and Technology [25]. The measured  $3s_{1/2} - 3p_{3/2}$  line positions, however, did not have the accuracies required to differentiate between theories.

In the present paper the wavelengths of the  $3s_{1/2} - 3p_{3/2}$  and  $3p_{1/2} - 3d_{3/2}$  resonance transitions in Na-, Mg-, Al-, and Si-like W ions are measured in high resolution together with the equivalent transitions from lower charge states down to K-like  $W^{55+}$ . The measured tungsten spectra have been analyzed using theoretical spectra calculated by using the Flexible Atomic Code (FAC) [26]. The FAC calculated  $3s_{1/2} - 3p_{3/2}$  wavelengths are compared with results from the General-purpose Relativistic Atomic Structure Program (GRASP2) [27, 28]. The measured line positions of the sodium- and magnesiumlike resonance transitions are evaluated with calculated wavelengths from several codes, including a recent result from RCI calculations [29].

## II. THEORY

The structure and spectra of calciumlike  $W^{54+}$  through fluorinelike  $W^{65+}$  ions have been calculated using FAC v.1.1.1 [26, 30]. The ions have been modeled with K-shell cores. Autoionization has been included for all charge states lower than neonlike from all levels to the ground and low-lying configurations of the daughter ion. Configuration state functions used in the FAC calculations are listed in Table I.

In addition, the  $\Delta n = 0$  M-shell transitions in K-like  $W^{55+}$  through Ne-like  $W^{64+}$  ions have also been calculated with GRASP2 [27, 28] using the EAL calculation mode. Included configuration state functions are tabulated in Table II. The theoretical  $3s_{1/2} - 3p_{3/2}$  wavelengths from FAC and GRASP2 are compared with experimental line positions in Fig. 1.

High-precision calculations of the sodiumlike  $3s_{1/2} - 3p_{3/2}$  line have been performed by Sapirstein *et al.* [29]. Here, the transition energy has been calculated by using the RCI and RMBPT codes and equal 537.51 eV including electron-correlation energy. To this energy corrections for mass polarization (-0.01 eV) and QED effects (-4.42 eV) have been added,

resulting in a total energy of 533.08(4) eV, where the uncertainty is estimated to be mainly due to the neglect of two-loop Lamb shifts and negative energy states. This transition energy corresponds to a wavelength of 23.258(2) Å.

### III. MEASUREMENT AND ANALYSIS

The experiment employed the SuperEBIT electron-beam ion trap at the Lawrence Livermore National Laboratory [31, 32]. Tungsten was supplied to the trap using a Metal Vapor Vacuum Arc (MeVVA) injector, which injects few-times ionized tungsten into SuperEBIT. Trapped by electric and magnetic fields the ions reached higher charge states under the bombardment by a narrow ( $\leq 60 \mu\text{m}$ ) electron beam of energy 23.5 keV and beam currents around 55 mA.

The spectrometer employed for the measurement was a very high resolution soft x-ray grating spectrometer [33]. The instrument uses a 2400 lines/mm spherical  $R = 44.3$  m grating operated at a grazing angle of  $2^\circ$ . The flat-field images were recorded using a cryogenically cooled Princeton Instruments charge-coupled device (CCD) detector. The back-illuminated CCD chip is made up of  $1300 \times 1340$  pixels, each of size  $20 \times 20 \mu$ . The spectrometer was set up to cover the 18.5 - 26.5 Å soft x-ray band. The instrument was not in best focus because of constraints placed on its use by other experiments before and after.

Nitrogen and carbon dioxide gases were supplied to the trap by a gas injector to provide accurate reference wavelengths in first order. A second-degree polynomial dispersion function of wavelength versus detector channel position was determined by using the theoretical line positions of N VII Ly- $\alpha$  and Ly- $\beta$ , N VI K $\beta$ , O VIII Ly- $\alpha$ , and O VII K $\alpha$  (w and z). The H-like wavelengths are taken from Garcia and Mack [34], the He-like K $\alpha$  lines from Drake [35], and the He-like K $\beta$  transition from Vainshtein and Safronova [36]. The wavelengths of the He-like ions are believed to be accurate to better than 0.6 mÅ [37]. The present measurement is thus similar to the measurement of the  $2s_{1/2} - 2p_{1/2}$  Li-like  $\text{U}^{89+}$  where the O VII lines were used as reference lines in second order [38].

Tungsten spectra were acquired during four days. The half-hour and one-hour exposure CCD images were rotated to correct for a slight tilt in the alignment of the CCD camera before the cosmic-ray and stray-light counts were filtered out, keeping only single photon counts. The data from each day were added and analyzed separately. The  $3s_{1/2} - 3p_{3/2}$

transitions in Na- and Mg-like W, and the  $3p_{1/2} - 3d_{3/2}$  in Al- and Si-like W were of sufficient strength so that they could be analyzed in each of these data sets. The wavelength dispersion determined from the nitrogen and oxygen spectra was applied to these tungsten spectra and anchored to the position of line w from He-like O VII, which showed in each spectrum, because oxygen existed in the trap as an impurity. The inferred line positions from all the data sets, see Fig. 2, were averaged to give the resulting wavelengths in Tables III - VI. The uncertainties in the four line positions were determined based on the counting statistics of each line in addition to the counting statistics associated with the O w reference line. Furthermore, the uncertainties in the line positions due to line blends were estimated for the Mg- and Si-like W lines. These uncertainties were added in quadrature for each data set and thereafter averaged. Then the reference-line uncertainty was added in quadrature followed by the linear addition of the dispersion uncertainty. The contributions to the line-position uncertainties are listed in Tables III - VI.

For the weaker tungsten lines the analysis was done after the four data sets had been summed, see Fig. 3. As with the individual data sets, the wavelength dispersion was anchored to the O w line position. To identify the lines, a synthetic spectrum was calculated for an electron energy of 23.5 keV and an electron density of  $5 \times 10^{11} \text{ cm}^{-3}$ . This spectrum is shown in Fig. 4, where the lines are modeled with an instrumental resolution of 40 mÅ full width at half maximum. The tungsten charge balance was estimated from the measured number of counts in the observed lines and the corresponding calculated line emissivities. The resulting charge balance relative the sodiumlike tungsten ion is shown in Fig. 5. The uncertainties in the abundances are difficult to estimate. For the ions with only a single line, the uncertainties are based on the statistics of the measured line intensities. For ions with several observed lines, the errors are estimated from both the counting statistics and the spread of the number of ions derived from each individual line. Comparing the experimental and theoretical spectra allowed for the identification of lines from potassiumlike through neonlike tungsten. Although no calciumlike lines were observed, the abundance of Ca-like  $\text{W}^{54+}$  was set equal to that of K-like  $\text{W}^{55+}$  to account for the maximum possible influence of line blends. To estimate line-blend effects, the centroid of each line was fitted in the theoretical one-charge state spectrum and in the synthetic spectrum where lines from all ions were present. The wavelength differences were taken as the blend errors. These uncertainties were added in quadrature with the statistics of each line and O w and the

reference-line uncertainty, followed by a linear addition of the dispersion uncertainty. All identified lines are listed in Table VII with experimental wavelengths and theoretical line positions from FAC and GRASP2. The three lines Cl-3, S-2, and P-1 have been identified in the theoretical model. However, because the line positions overlap, a determination of these experimental wavelengths is not possible.

Constants used are  $hc = 12398.42 \text{ \AA}\cdot\text{eV} = 8065.5410 \text{ eV}\cdot\text{cm}$  and  $1 \text{ Ry} = 13.60569 \text{ eV}$ .

#### IV. SUMMARY AND CONCLUSION

The measurement yields wavelengths for 20 soft x-ray  $\Delta n = 0$  M-shell lines in highly charged tungsten ions between 19 and 25  $\text{\AA}$ , see Table VII and Fig. 3. Lines from potassiumlike  $\text{W}^{55+}$  to neonlike  $\text{W}^{64+}$  are measured in high resolution and identified using theoretical spectra calculated using FAC, cf. Fig. 4. Comparisons with FAC and GRASP2 calculations are made for the  $3s_{1/2} - 3p_{3/2}$  transitions in K-like  $\text{W}^{55+}$  through Ne-like  $\text{W}^{64+}$  ions, see Fig. 1. The comparison shows that our FAC calculations on average do a better job in reproducing the measured values than our GRASP2 calculations. Both do poorly for the neonlike line, cf. previous work on the  $2s_{1/2} - 2p_{3/2}$  transitions in Li-like  $\text{Th}^{80+}$  and  $\text{U}^{82+}$  [39, 40]. Overall the theoretical wavelengths are too short, but not consistently.

Several calculations have been made for the resonance line in sodiumlike ions and the observed  $3s_{1/2} - 3p_{3/2}$  tungsten line position is compared with these in Fig. 6, where sodiumlike ions with  $70 \leq Z \leq 80$  are shown. The experimental wavelength of  $23.253(5) \text{ \AA}$  agrees well with the *ab initio* calculations by Kim *et al.* [2], Blundell [11], and the new *ab initio* value by Sapirstein *et al.* [29]. The latter comparison is shown in Table VII. The calculations by Kim *et al.* [2] and Blundell [11] are also in good agreement with the high-precision measurement of Na-like  $\text{Pt}^{67+}$  by Cowan *et al.* [20] performed at the Livermore EBIT-II electron-beam ion trap.

A comparison between measurements and theory of the magnesiumlike resonance line displayed in Fig. 7 shows that the measured Mg-like  $\text{W}^{62+}$  wavelength of  $22.735(4)$  does not agree with available theoretical predictions. This contrasts with the measurement by Gillaspay *et al.* [25], whose larger error bars show consistency with the two calculations. We note that the predictions from the MCDF [12], RRPA [13], and model-potential relativistic perturbation theory [14] codes are off the scale and, therefore, not shown in Fig. 7. Mag-



nesiumlike ions are more difficult to calculate with accuracy and additional high-precision measurements of the  $3s^2 - 3s_{1/2}3p_{3/2}$  transition in high- $Z$  ions are needed to guide theory.

## ACKNOWLEDGMENTS

This work was performed under the auspices of the United States Department of Energy by Lawrence Livermore National Laboratory under Contract DE-AC52-07NA27344. The authors would like to thank Todd Chambers, Miriam Frankel, Dr. Jaan Lepson, Debbie Miller, Yuri Podpaly, Ed Magee, and Prof. Elmar Träbert for assistance with the measurement. The authors furthermore would like to thank Dr. K. T. Cheng, Dr. Mau Chen, and Dr. Jonathan Sapirstein for making unpublished results available. Joel Clementson would like to thank Dr. Hans Lundberg, Dr. Sven Hultdt, Prof. Sune Svanberg, and Prof. Tomas Brage for their support.

- 
- [1] I. Martinson, Nucl. Instr. and Meth. B **43**, 323 (1989).
  - [2] Y.-K. Kim, D. H. Baik, P. Indelicato, and J. P. Deslaux, Phys. Rev. A **44**, 148 (1991).
  - [3] K. T. Cheng, M. H. Chen, W. R. Johnson, and J. Sapirstein, Can. J. Phys. **86**, 33 (2008).
  - [4] P. Beiersdorfer, J. Phys. B: At. Mol. Opt. Phys. (2010), accepted.
  - [5] L. N. Ivanov and E. P. Ivanova, At. Data Nucl. Data Tables **24**, 95 (1979).
  - [6] Y.-K. Kim and K.-T. Cheng, J. Opt. Soc. Am. **68**, 836 (1978).
  - [7] W. R. Johnson, S. A. Blundell, and J. Sapirstein, Phys. Rev. A **38**, 2699 (1988).
  - [8] J. F. Seely and R. A. Wagner, Phys. Rev. A **41**, 5246 (1990).
  - [9] D. H. Baik, Y. G. Ohr, K. S. Kim, J. M. Lee, P. Indelicato, and Y.-K. Kim, At. Data Nucl. Data Tables **47**, 177 (1991).
  - [10] J. F. Seely, C. M. Brown, U. Feldman, J. O. Ekberg, C. J. Keane, B. J. MacGowan, D. R. Kania, and W. E. Behring, At. Data Nucl. Data Tables **47**, 1 (1991).
  - [11] S. A. Blundell, Phys. Rev. A **47**, 1790 (1993).
  - [12] K. T. Cheng and W. R. Johnson, Phys. Rev. A **16**, 263 (1977).
  - [13] P. Shorer, C. D. Lin, and W. R. Johnson, Phys. Rev. A **16**, 1109 (1977).
  - [14] E. P. Ivanova, L. N. Ivanov, and M. A. Tsirekidze, At. Data Nucl. Data Tables **35**, 419 (1986).

- [15] J. P. Marques, F. Parente, and P. Indelicato, *At. Data Nucl. Data Tables* **55**, 157 (1993).
- [16] M. H. Chen and K. T. Cheng, *Phys. Rev. A* **55**, 3440 (1997).
- [17] Y. Zou and C. Froese Fischer, *J. Phys. B: At. Mol. Opt. Phys.* **34**, 915 (2001).
- [18] J. F. Seely, U. Feldman, C. M. Brown, M. C. Richardson, D. D. Dietrich, and W. E. Behring, *J. Opt. Soc. Am. B* **5**, 785 (1988).
- [19] E. Träbert, P. Beiersdorfer, J. K. Lepson, and H. Chen, *Phys. Rev. A* **68**, 042501 (2003).
- [20] T. E. Cowan, C. L. Bennett, D. D. Dietrich, J. V. Bixler, C. J. Hailey, J. R. Henderson, D. A. Knapp, M. A. Levine, R. E. Marrs, and M. B. Schneider, *Phys. Rev. Lett.* **66**, 1150 (1991).
- [21] A. Simionovici, D. D. Dietrich, R. Keville, T. Cowan, P. Beiersdorfer, M. H. Chen, and S. A. Blundell, *Phys. Rev. A* **48**, 3056 (1993).
- [22] P. Beiersdorfer and B. J. Wargelin, *Rev. Sci. Instrum.* **65**, 13 (1994).
- [23] P. Beiersdorfer, E. Träbert, H. Chen, M. J. May, and A. L. Osterheld, *Phys. Rev. A* **67**, 052103 (2003).
- [24] M. H. Chen, K. T. Cheng, P. Beiersdorfer, and J. Sapirstein, *Phys. Rev. A* **68**, 022507 (2003).
- [25] J. D. Gillaspay, I. N. Draganić, Y. Ralchenko, J. Reader, J. N. Tan, J. M. Pomeroy, and S. M. Brewer, *Phys. Rev. A* **80**, 010501(R) (2009).
- [26] M. F. Gu, *Can. J. Phys.* **86**, 675 (2008).
- [27] K. G. Dyall, I. P. Grant, C. T. Johnson, F. A. Parpia, and E. P. Plummer, *Comput. Phys. Commun.* **55**, 425 (1989).
- [28] F. A. Parpia, I. P. Grant, and C. Froese Fischer, unpublished.
- [29] J. Sapirstein, M. H. Chen, and K. T. Cheng (2009), private communication.
- [30] M. F. Gu, *AIP Conf. Proc.* **730**, 127 (2004).
- [31] D. A. Knapp, R. E. Marrs, S. R. Elliott, E. W. Magee, and R. Zasadzinski, *Nucl. Instr. and Meth. A* **334**, 305 (1993).
- [32] P. Beiersdorfer, *Can. J. Phys.* **86**, 1 (2008).
- [33] P. Beiersdorfer, E. W. Magee, E. Träbert, H. Chen, J. K. Lepson, M.-F. Gu, and M. Schmidt, *Rev. Sci. Instrum.* **75**, 3723 (2004).
- [34] J. D. Garcia and J. E. Mack, *J. Opt. Soc. Am.* **55**, 654 (1965).
- [35] G. W. Drake, *Can. J. Phys.* **66**, 586 (1988).
- [36] L. A. Vainshtein and U. I. Safronova, *Phys. Scr.* **31**, 519 (1985).
- [37] L. Engström and U. Litzen, *J. Phys. B: At. Mol. Opt. Phys.* **28**, 2565 (1995).

- [38] P. Beiersdorfer, H. Chen, D. B. Thorn, and E. Träbert, Phys. Rev. Lett. **95**, 233003 (2005).
- [39] P. Beiersdorfer, A. Osterheld, S. R. Elliott, M. H. Chen, D. Knapp, and K. Reed, Phys. Rev. A **52**, 2693 (1995).
- [40] P. Beiersdorfer, D. Knapp, R. E. Marrs, S. R. Elliott, and M. H. Chen, Phys. Rev. Lett. **71**, 3939 (1993).

TABLE I: Configuration state functions used in the FAC calculations with K-shell core.

$l = 0, 1, \dots, n - 1; l^* = s, p; n = 3, 4, 5; n^* = 4, 5$

F-like W <sup>65+</sup>	Ne-like W <sup>64+</sup>	Na-like W <sup>63+</sup>	Mg-like W <sup>62+</sup>
2s <sup>2</sup> 2p <sup>5</sup>	2s <sup>2</sup> 2p <sup>6</sup>	2s <sup>2</sup> 2p <sup>6</sup> nl	2s <sup>2</sup> 2p <sup>6</sup> 3lnl
2s2p <sup>6</sup>	2s <sup>2</sup> 2p <sup>5</sup> nl	2s <sup>2</sup> 2p <sup>5</sup> 3lnl	2s <sup>2</sup> 2p <sup>5</sup> 3l3lnl
2s <sup>2</sup> 2p <sup>4</sup> nl	2s2p <sup>6</sup> nl	2s2p <sup>6</sup> 3lnl	2s2p <sup>6</sup> 3l3lnl
2s2p <sup>5</sup> nl			
2p <sup>6</sup> nl			
Al-like W <sup>61+</sup>	Si-like W <sup>60+</sup>	P-like W <sup>59+</sup>	S-like W <sup>58+</sup>
2s <sup>2</sup> 2p <sup>6</sup> 3l3lnl	2s <sup>2</sup> 2p <sup>6</sup> 3l3l3lnl	2s <sup>2</sup> 2p <sup>6</sup> 3l3l3l3l3l	2s <sup>2</sup> 2p <sup>6</sup> 3l3l3l3l3l3l
2s <sup>2</sup> 2p <sup>5</sup> 3s <sup>2</sup> 3l3l	2s <sup>2</sup> 2p <sup>5</sup> 3s <sup>2</sup> 3l3l3l	2s <sup>2</sup> 2p <sup>6</sup> 3l*3l*3l*3ln*l	2s <sup>2</sup> 2p <sup>6</sup> 3l*3l*3l*3l*3ln*l
2s <sup>2</sup> 2p <sup>5</sup> 3l*3l*3l*n*l	2s <sup>2</sup> 2p <sup>5</sup> 3l*3l*3l*n*l	2s <sup>2</sup> 2p <sup>5</sup> 3s <sup>2</sup> 3p <sup>3</sup> nl	2s <sup>2</sup> 2p <sup>5</sup> 3s <sup>2</sup> 3p <sup>4</sup> nl
2s2p <sup>6</sup> 3s <sup>2</sup> 3l3l	2s2p <sup>6</sup> 3s <sup>2</sup> 3l3l3l	2s2p <sup>6</sup> 3s <sup>2</sup> 3p <sup>3</sup> nl	2s2p <sup>6</sup> 3s <sup>2</sup> 3p <sup>4</sup> nl
2s2p <sup>6</sup> 3l*3l*3l*n*l	2s2p <sup>6</sup> 3l*3l*3l*n*l		
Cl-like W <sup>57+</sup>	Ar-like W <sup>56+</sup>	K-like W <sup>55+</sup>	Ca-like W <sup>54+</sup>
2s <sup>2</sup> 2p <sup>6</sup> 3l3l3l3l3l3l	2s <sup>2</sup> 2p <sup>6</sup> 3l*3l*3l*3l3l3l3l	2s <sup>2</sup> 2p <sup>6</sup> 3l*3l*3l*3l3l3l3l3l	2s <sup>2</sup> 2p <sup>6</sup> 3l*3l*3l*3l3l3l3l3l3l
2s <sup>2</sup> 2p <sup>6</sup> 3l*3l*3l*3l*3l*3ln*l	2s <sup>2</sup> 2p <sup>6</sup> 3l*3l*3l*3l*3l*3ln*l	2s <sup>2</sup> 2p <sup>6</sup> 3l*3l*3l*3l*3l*3ln*l	2s <sup>2</sup> 2p <sup>6</sup> 3l*3l*3l*3l*3l*3ln*l
2s <sup>2</sup> 2p <sup>5</sup> 3s <sup>2</sup> 3p <sup>5</sup> nl	2s <sup>2</sup> 2p <sup>5</sup> 3s <sup>2</sup> 3p <sup>6</sup> nl	2s <sup>2</sup> 2p <sup>5</sup> 3s <sup>2</sup> 3p <sup>6</sup> 3dnl	2s <sup>2</sup> 2p <sup>5</sup> 3s <sup>2</sup> 3p <sup>6</sup> 3d <sup>2</sup> nl
2s2p <sup>6</sup> 3s <sup>2</sup> 3p <sup>5</sup> nl	2s2p <sup>6</sup> 3s <sup>2</sup> 3p <sup>6</sup> nl	2s2p <sup>6</sup> 3s <sup>2</sup> 3p <sup>6</sup> 3dnl	2s2p <sup>6</sup> 3s <sup>2</sup> 3p <sup>6</sup> 3d <sup>2</sup> nl

TABLE II: Configuration state functions used in the GRASP2 calculations with filled K shell (Ne-like W) and L shell (Na- through K-like W).

Ne-like W <sup>64+</sup>	Na-like W <sup>63+</sup>	Mg-like W <sup>62+</sup>	Al-like W <sup>61+</sup>	Si-like W <sup>60+</sup>
2s <sup>2</sup> 2p <sup>6</sup>	3s	3s <sup>2</sup>	3s <sup>2</sup> 3p	3s <sup>2</sup> 3p <sup>2</sup>
2s <sup>2</sup> 2p <sup>5</sup> 3s	3p	3s3p	3s <sup>2</sup> 3d	3s <sup>2</sup> 3p3d
2s <sup>2</sup> 2p <sup>5</sup> 3p	3d	3s3d	3s3p <sup>2</sup>	3s <sup>2</sup> 3d <sup>2</sup>
2s <sup>2</sup> 2p <sup>5</sup> 3d			3s3p3d	3s3p <sup>3</sup>
2s2p <sup>6</sup> 3s				3s3p <sup>2</sup> 3d
2s2p <sup>6</sup> 3p				3s3p3d <sup>2</sup>
2s2p <sup>6</sup> 3d				
P-like W <sup>59+</sup>	S-like W <sup>58+</sup>	Cl-like W <sup>57+</sup>	Ar-like W <sup>56+</sup>	K-like W <sup>55+</sup>
3s <sup>2</sup> 3p <sup>3</sup>	3s <sup>2</sup> 3p <sup>4</sup>	3s <sup>2</sup> 3p <sup>5</sup>	3s <sup>2</sup> 3p <sup>6</sup>	3s <sup>2</sup> 3p <sup>6</sup> 3d
3s <sup>2</sup> 3p <sup>2</sup> 3d	3s <sup>2</sup> 3p <sup>3</sup> 3d	3s <sup>2</sup> 3p <sup>4</sup> 3d	3s <sup>2</sup> 3p <sup>5</sup> 3d	3s <sup>2</sup> 3p <sup>5</sup> 3d <sup>2</sup>
3s3p <sup>4</sup>	3s3p <sup>5</sup>	3s3p <sup>6</sup>	3s3p <sup>6</sup> 3d	3s3p <sup>6</sup> 3d <sup>2</sup>
3s3p <sup>3</sup> 3d	3s3p <sup>4</sup> 3d	3s3p <sup>5</sup> 3d		

TABLE III: Measured positions of the Na-like  $W^{63+}$   $3s_{1/2} - 3p_{3/2}$  transition, error contributions, and average wavelength. Wavelengths in Å.

Data set	1	2	3	4
Wavelength	23.2556	23.2568	23.2562	23.2466
Statistics	0.0015	0.0015	0.0022	0.0016
O w statistics	0.0023	0.0036	0.0039	0.0027
Reference	0.0006			
Dispersion	0.0031			
Result	$23.253 \pm 0.005$			

TABLE IV: Measured positions of the Mg-like  $W^{62+}$   $3s_{1/2} - 3p_{3/2}$  transition, error contributions, and average wavelength. Wavelengths in Å.

Data set	1	2	3	4
Wavelength	22.7377	22.7391	22.7379	22.7299
Statistics	0.0016	0.0015	0.0023	0.0015
O w statistics	0.0023	0.0036	0.0039	0.0027
Line blend	0.0023	0.0026		0.0017
Reference	0.0006			
Dispersion	0.0022			
Result	$22.735 \pm 0.004$			

TABLE V: Measured positions of the Al-like  $W^{61+}$   $3p_{1/2} - 3d_{3/2}$  transition, error contributions, and average wavelength. Wavelengths in Å.

Data set	1	2	3	4
Wavelength	20.7544	20.7608	20.7581	20.7533
Statistics	0.0021	0.0025	0.0034	0.0021
O w statistics	0.0023	0.0036	0.0039	0.0027
Reference	0.0006			
Dispersion	0.0017			
Result	$20.756 \pm 0.004$			

TABLE VI: Measured positions of the Si-like  $W^{60+}$   $3p_{1/2} - 3d_{3/2}$  transition, error contributions, and average wavelength. Wavelengths in Å.

Data set	1	2	3	4
Wavelength	20.2681	20.2708	20.2730	20.2673
Statistics	0.0021	0.0029	0.0030	0.0018
O w statistics	0.0023	0.0036	0.0039	0.0027
Line blend	0.0031	0.0093		0.0049
Reference	0.0006			
Dispersion	0.0026			
Result	$20.270 \pm 0.005$			

TABLE VII: Experimental and theoretical tungsten wavelengths in Å. The lines are labeled according to charge state, cf. Fig. 3. Theory from FAC, GRASP2, and RCI [29] calculations.

Key	Transition	Experiment	FAC	GRASP2	RCI
K-1	$(3s^2 3p^6 3d_{3/2})_{3/2} - (3s^2 3p_{1/2} 3p_{3/2}^4 3d_{3/2}^2)_{3/2}$	19.184(8)	19.143	19.078	
Cl-1	$(3s^2 3p_{1/2}^2 3p_{3/2}^3)_{3/2} - (3s^2 3p_{1/2} 3p_{3/2}^3 3d_{3/2})_{1/2}$	19.62(1)	19.570	19.442	
Ar-1	$(3s^2 3p^6)_0 - (3s^2 3p_{1/2} 3p_{3/2}^4 3d_{3/2})_1$	19.679(7)	19.636	19.607	
S-1	$(3s^2 3p_{1/2}^2 3p_{3/2}^2)_{2/2} - (3s^2 3p_{1/2} 3p_{3/2}^2 3d_{3/2})_1$	19.752(8)	19.702	19.592	
Cl-2	$(3s^2 3p_{1/2}^2 3p_{3/2}^3)_{3/2} - (3s^2 3p_{1/2} 3p_{3/2}^3 3d_{3/2})_{3/2}$	19.814(9)	19.786	19.726	
Cl-3	$(3s^2 3p_{1/2}^2 3p_{3/2}^3)_{3/2} - (3s^2 3p_{1/2} 3p_{3/2}^3 3d_{3/2})_{5/2}$		19.867	19.789	
S-2	$(3s^2 3p_{1/2}^2 3p_{3/2}^2)_{2/2} - (3s^2 3p_{1/2} 3p_{3/2}^2 3d_{3/2})_{2/2}$		19.883	19.755	
	$(3s^2 3p_{1/2}^2 3p_{3/2}^2)_0 - (3s^2 3p_{1/2} 3p_{3/2}^2 3d_{3/2})_1$		19.922	19.852	
P-1	$(3s^2 3p_{1/2}^2 3p_{3/2})_{3/2} - (3s^2 3p_{1/2} 3p_{3/2} 3d_{3/2})_{3/2}$		19.916	19.789	
	$(3s^2 3p_{1/2}^2 3p_{3/2})_{3/2} - (3s^2 3p_{1/2} 3p_{3/2} 3d_{3/2})_{1/2}$		19.942	19.846	
S-3	$(3s^2 3p_{1/2}^2 3p_{3/2}^2)_{2/2} - (3s^2 3p_{1/2} 3p_{3/2}^2 3d_{3/2})_3$	20.147(6)	20.116	20.006	
Si-1	$(3s^2 3p_{1/2}^2)_0 - (3s^2 3p_{1/2} 3d_{3/2})_1$	20.270(5)	20.229	20.200	
P-2	$(3s^2 3p_{1/2}^2 3p_{3/2})_{3/2} - (3s^2 3p_{1/2} 3p_{3/2} 3d_{3/2})_{5/2}$	20.319(5)	20.285	20.187	
K-2	$(3s^2 3p^6 3d_{3/2})_{3/2} - (3s^2 3p_{1/2} 3p_{3/2}^4 3d_{3/2}^2)_{5/2}$	20.552(7)	20.536	20.575	
Al-1	$(3s^2 3p_{1/2})_{1/2} - (3s^2 3d_{3/2})_{3/2}$	20.756(4)	20.721	20.637	
Ne-1	$(2s^2 2p_{1/2}^2 2p_{3/2}^3 3s_{1/2})_1 - (2s^2 2p_{1/2}^2 2p_{3/2}^3 3p_{3/2})_0$	21.085(6)	20.969	20.975	
Mg-1	$(3s_{1/2} 3p_{1/2})_1 - (3s_{1/2} 3d_{3/2})_2$	21.372(6)	21.360	21.622	
Al-2	$(3s^2 3p_{1/2})_{1/2} - (3s_{1/2} 3p_{1/2} 3p_{3/2})_{1/2}$	22.543(4)	22.506	22.430	
Mg-2	$(3s^2)_0 - (3s_{1/2} 3p_{3/2})_1$	22.735(4)	22.701	22.755	
Si-2	$(3s^2 3p_{1/2}^2)_0 - (3s_{1/2} 3p_{1/2}^2 3p_{3/2})_1$	22.793(5)	22.766	22.764	
Al-3	$(3s^2 3p_{1/2})_{1/2} - (3s_{1/2} 3p_{1/2} 3p_{3/2})_{3/2}$	22.961(6)	22.950	22.855	
Na-1	$3s_{1/2} - 3p_{3/2}$	23.253(5)	23.237	23.245	23.258(2)
S-4	$(3s^2 3p_{1/2}^2 3p_{3/2}^2)_{2/2} - (3s_{1/2} 3p_{1/2}^2 3p_{3/2}^3)_{2/2}$	23.35(1)	23.345	23.247	
P-3	$(3s^2 3p_{1/2}^2 3p_{3/2})_{3/2} - (3s_{1/2} 3p_{1/2}^2 3p_{3/2}^2)_{5/2}$	24.042(9)	24.038	23.997	
Al-4	$(3s^2 3p_{1/2})_{1/2} - (3s_{1/2} 3p_{1/2} 3p_{3/2})_{3/2}$	24.78(1)	24.770	24.814	

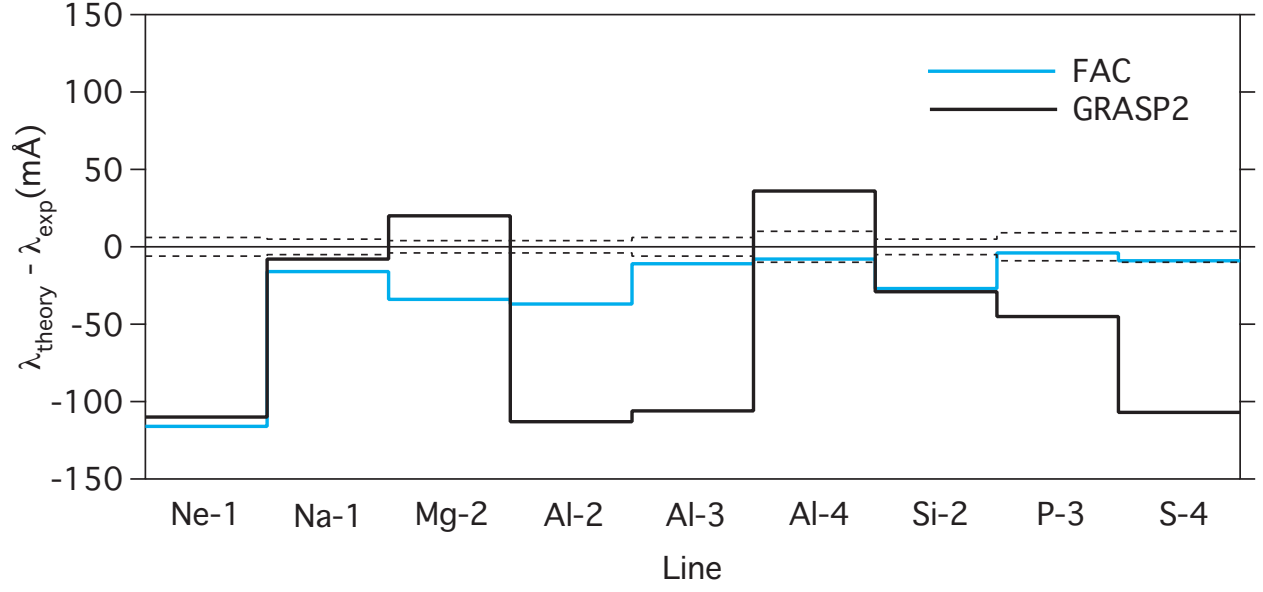


FIG. 1: Differences between theoretical  $3s_{1/2} - 3p_{3/2}$  FAC and GRASP2 wavelengths and observed line positions in highly charged tungsten ions. Experimental uncertainties are marked with dashed lines.



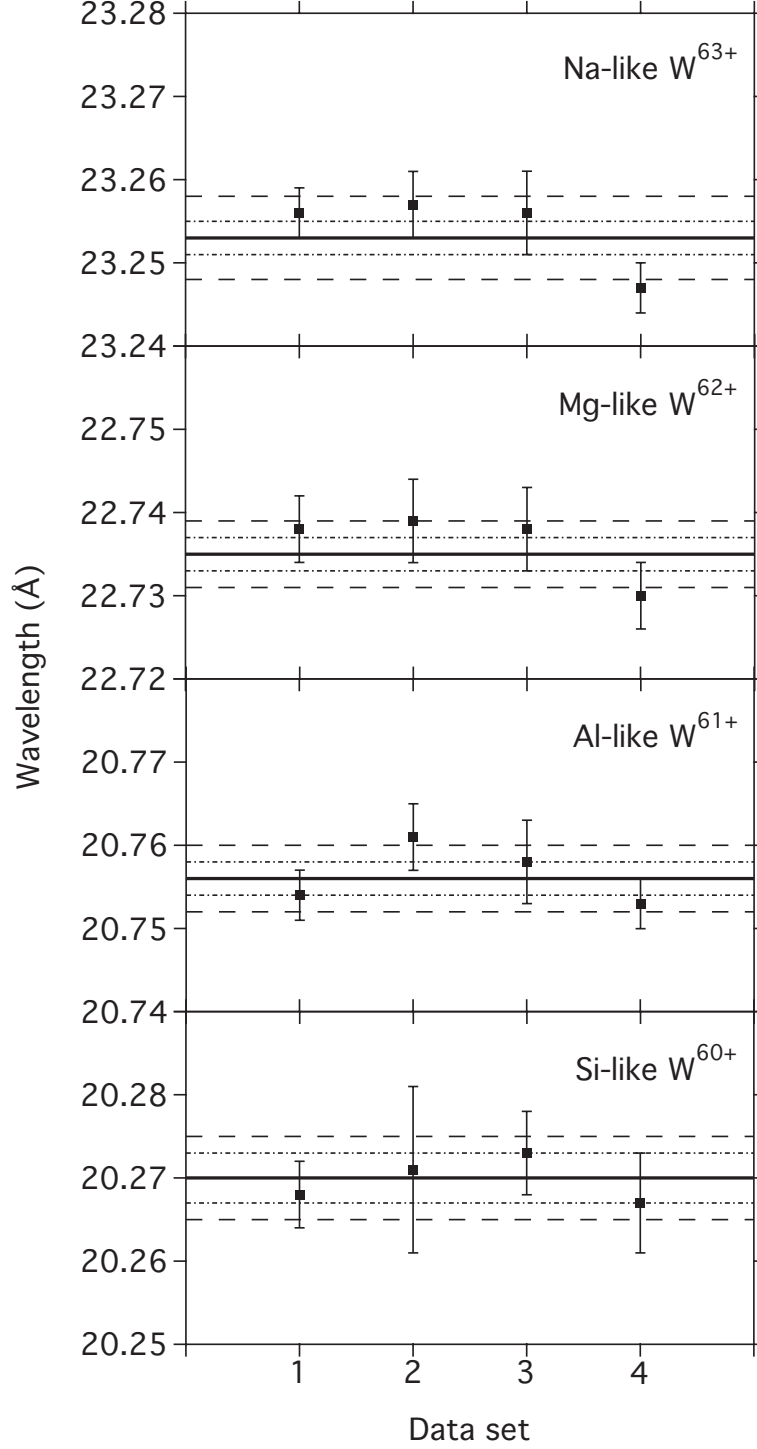


FIG. 2: Wavelengths of the Na-like through Si-like W resonance lines in the four data sets. The solid lines display the average wavelengths. Dashed lines represent the statistical and line-blend error bars, and the long dashed lines show the final wavelength uncertainties.

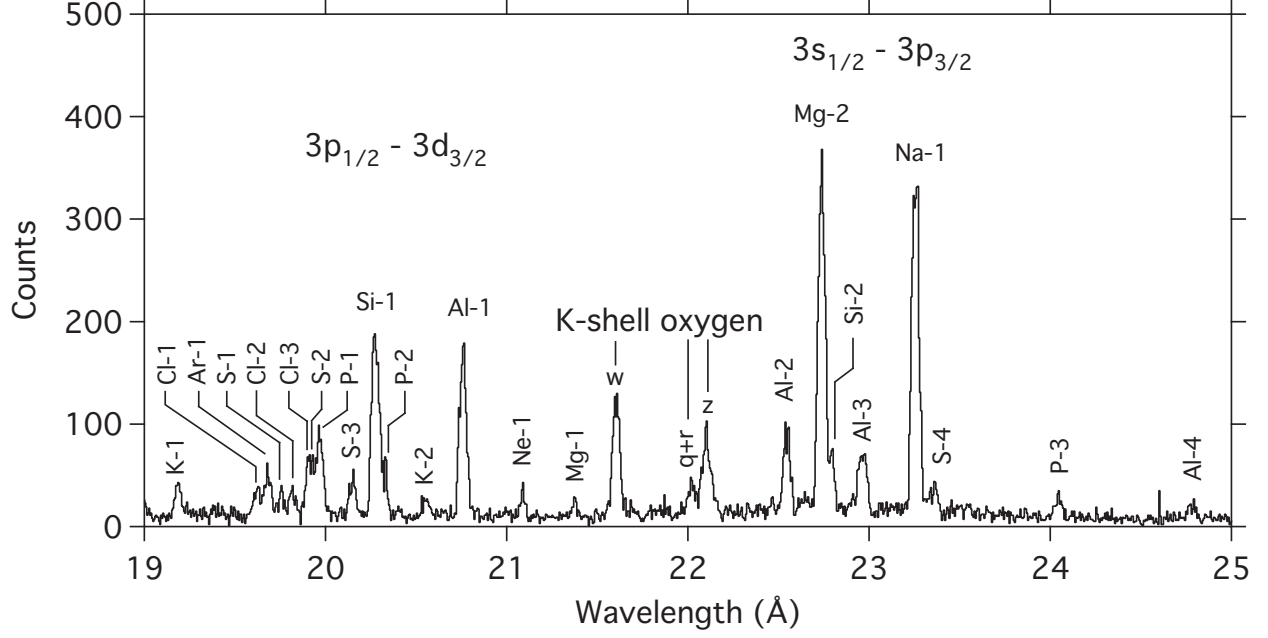


FIG. 3: Soft x-ray spectrum of highly charged tungsten measured with an  $R = 44.3$  m grazing-incidence spectrometer at the Livermore SuperEBIT electron-beam ion trap. The spectrum represents the co-added data from four run days.

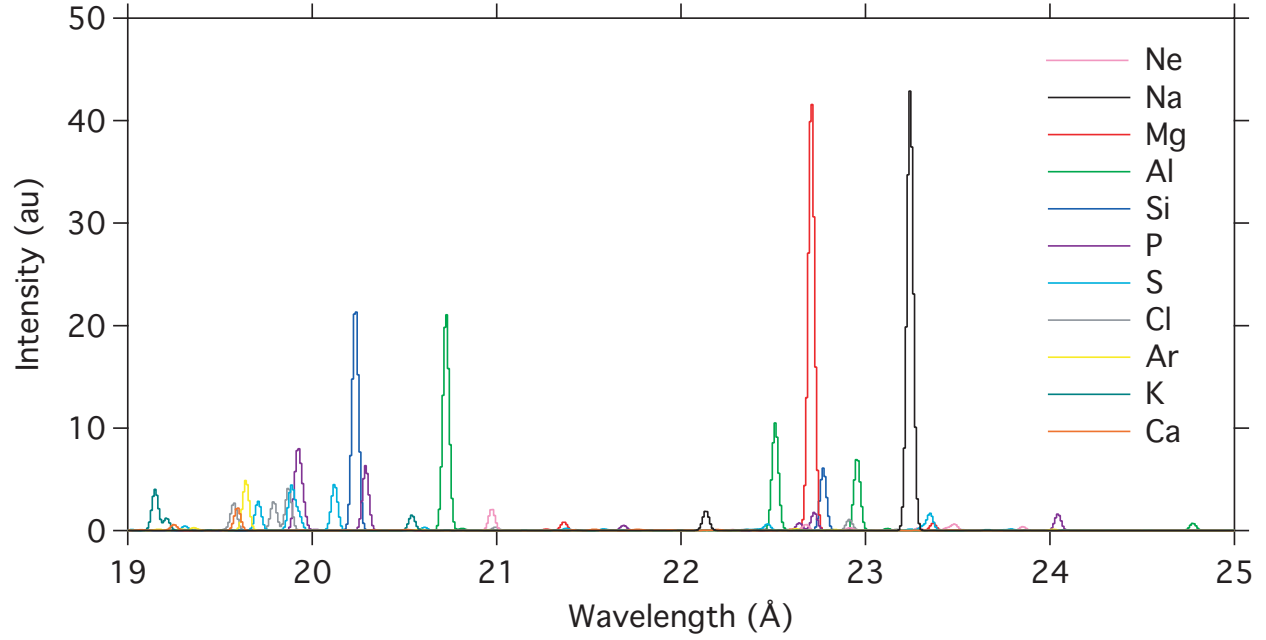


FIG. 4: Theoretical soft x-ray spectrum of highly charged tungsten. The spectrum is modeled with a resolution of 40 mÅ FWHM at an electron energy of 23.5 keV and a density of  $5 \times 10^{11} \text{ cm}^{-3}$ . The charge balance is inferred from the best agreement with the spectral data in Fig. 3 and is shown in Fig. 5.

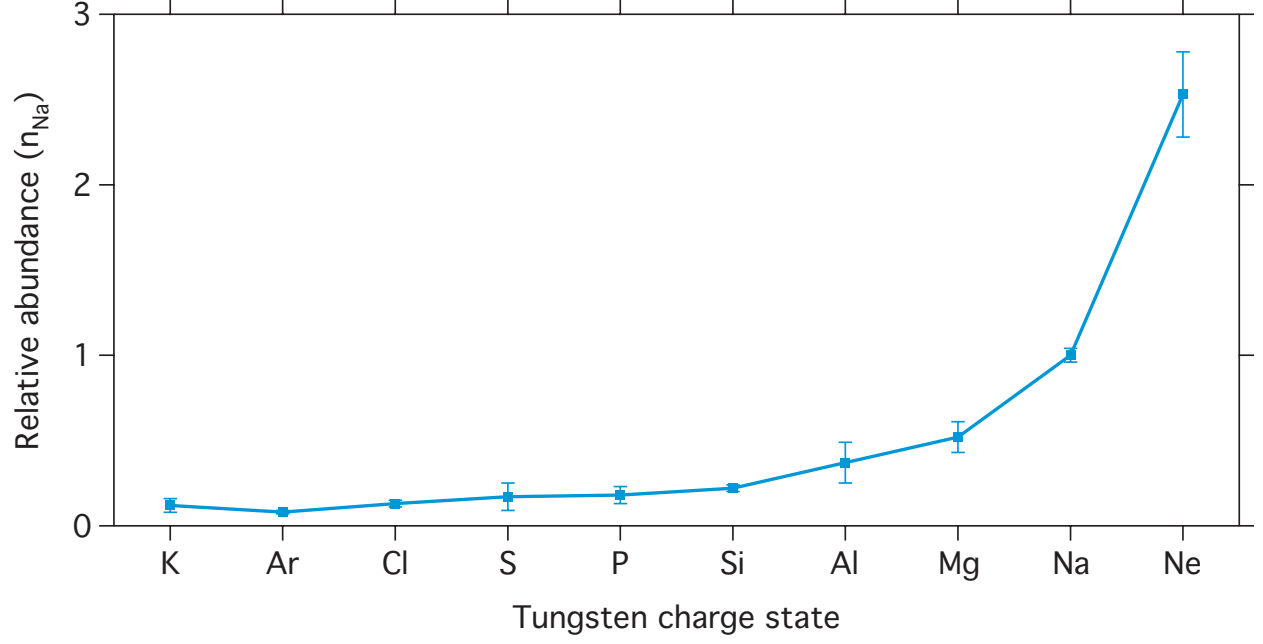


FIG. 5: Inferred tungsten charge state distribution in SuperEBIT at an electron-beam energy of  $E_b = 23.5$  keV. The charge state fractions are normalized to that of Na-like  $\text{W}^{63+}$ .

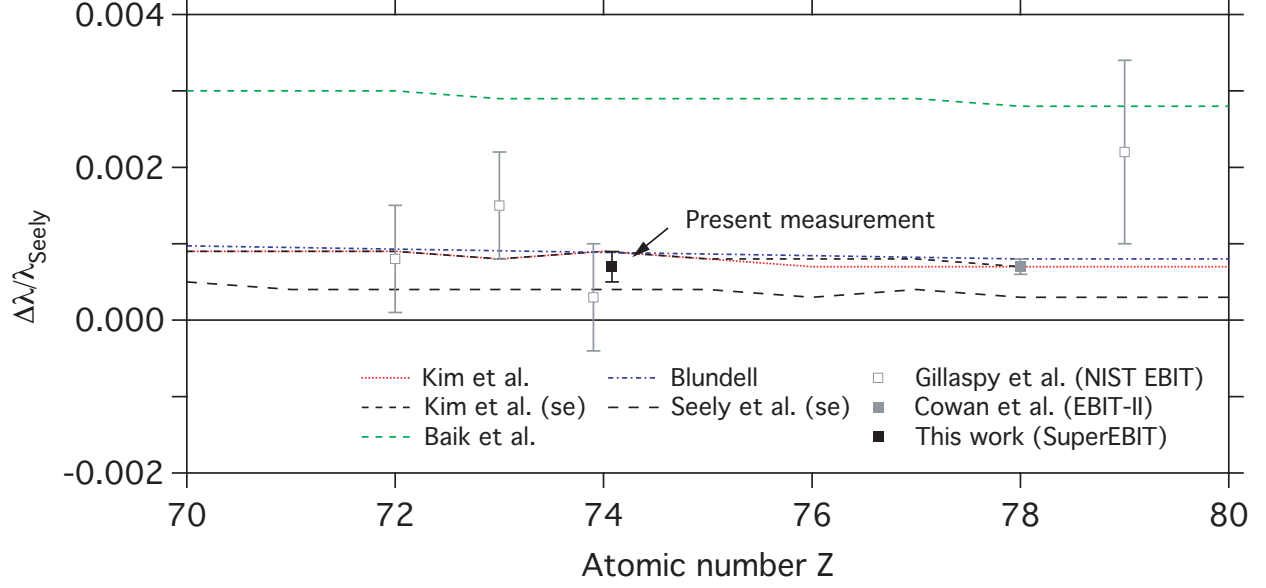


FIG. 6: Observed  $3s_{1/2} - 3p_{3/2}$  line positions of Na-like high- $Z$  ions [20, 25] compared to theoretical line positions by Kim *et al.* [2], Baik *et al.* [9], Blundell [11] and to semi-empirical (se) values by Kim *et al.* [2] and Seely *et al.* [8, 10]. Wavelengths are normalized to the theory by Seely *et al.* [10]. Note that the wavelengths by Blundell have been interpolated. Calculations from Johnson *et al.* [7], Ivanov and Ivanova [5], and Kim and Cheng [6] are off the scale. Observed values are from measurements at the NIST EBIT [25], the Livermore EBIT-II [20], and the Livermore SuperEBIT (this work).

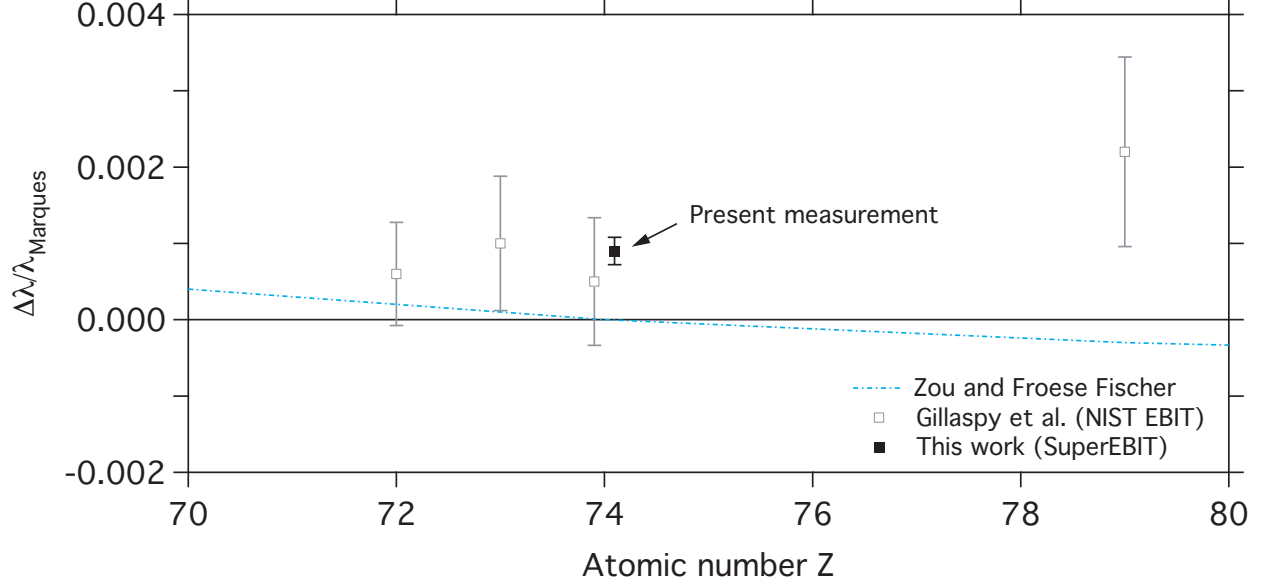


FIG. 7: Observed  $3s^2 - 3s_{1/2}3p_{3/2}$  line positions of Mg-like high- $Z$  ions compared to theoretical line positions by Zou and Froese Fischer [17]. Wavelengths are normalized to the theory by Marques *et al.* [15]. Note that wavelengths by Zou and Froese Fischer have been interpolated. Predictions from Cheng and Johnson [12], Shorer *et al.* [13], and Ivanova *et al.* [14] are off the scale. The experimental data are from the NIST EBIT [25] and the Livermore SuperEBIT (present work).